Fully Automated Soft Contact Lens Detection from NIR Iris Images

Balender Kumar[1], Aditya Nigam[2] and Phalguni Gupta[3]
[1]*Department of Computer Science and Engineering, Indian Institute of Technology Kanpur (IITK), Kanpur, India*
[2]*School of Computer Science and Electrical Engineering, Indian Institute of Technology Mandi (IIT Mandi), Mandi, India*
[3]*National Institute of Technical Teacher's & Research (NITTTR), Salt Lake, Kolkata, India*

Keywords: Iris, Contact Lens, Hough Transform, Soft Contact Lens, Multi-scale Line Tracking.

Abstract: Iris is considered as one of the best biometric trait for human authentication due to its accuracy and permanence. However easy iris spoofing raise the risk of false acceptance or false rejection. Recent iris recognition research has made an attempt to quantify the performance degradation due to the use of contact lens. This study proposes a strategy to detect soft contact lens in visual pictures of the eye obtained using NIR sensor. The lens border is detected by considering small annular ring-like area near the outer iris boundary and locating candidate points while traversing along the lens perimeter. The system performance is evaluated over public databases such as IIITD-Cogent, UND 2010, IIITD-Vista along with our self created IITK database. The rigorous experimentation revels the superior performance of the proposed system as compared with other existing techniques.

1 INTRODUCTION

In present world scenario, with bigger threats to the whole human race by several terrorist organizations around the world, ensuring human security is a huge challenge. Therefore automated human identification and verification are the basic requirements in order to provide secure and restricted access. There are several ways by which it can be realized such as token and knowledge based, but they can be very easily lost or circumvented. Several biometrics based solution has now been deployed to ensure robust and accurate human identification and verification. Many physiological biometric traits such as face, palmprint (Nigam and Gupta, 2014b), knuckleprint (Badrinath et al., 2011; Nigam and Gupta, 2011), fingerprint, face, iris (Nigam and Gupta, 2012), ear (Nigam and Gupta, 2014c) are well suited hence studied extensively. But it is observed that no trait can adequately support and deliver a system with desired performance. Hence recently many multimodal systems are proposed (Nigam and Gupta, 2015), (Nigam and Gupta, 2014a), (Nigam and Gupta, 2013a) suggesting different combinations of knuckleprint, iris, palmprint images in order to achieve better accuracy.

Image quality is another key factor which is very relevant in such systems but its computation is very difficult as its a very subjective task. Not much work is reported, investigating the quality of iris (Nigam et al., 2013), knuckleprint (Nigam and Gupta, 2013b) and palmprint images.

Out of all the available biometric traits, arguably iris can be considered as one of the best biometric trait for human authentication process, as it contain highly distinguishable texture (Flom and Safir, 1987). Also iris pattern remain unchanged after the age of two and does not degrade over time and environment. Performance wise it is best but it is vulnerable to spoofing via printed contact lenses. Also the system performance degrades severely while subjects wear contact lens (Lovish et al., 2015; Yadav et al., 2014; Kohli et al., 2013). Contact lenses are of two types cosmetic contact lens and Non-cosmetic or soft contact lens. Soft contact lens detection is an important and challenging problem to preventing spoofing as compared to cosmetic lens due to absence of any extra texture. Very limited amount of work is done in this area. In this work we deal with detection of soft contact lens based on faint edge detection using line tracking.

There are some techniques available to detect cosmetic contact lens which is easier to discriminate. Soft contact lens are texture-less and transparent hence are very difficult to differentiate. Most of the time they are unrecognizable even by humans in NIR images. The sole available clues are faintly visible lens boundaries. Thermal images has been used

Kumar, B., Nigam, A. and Gupta, P.
Fully Automated Soft Contact Lens Detection from NIR Iris Images.
DOI: 10.5220/0005702005890596
In *Proceedings of the 5th International Conference on Pattern Recognition Applications and Methods (ICPRAM 2016)*, pages 589-596
ISBN: 978-989-758-173-1

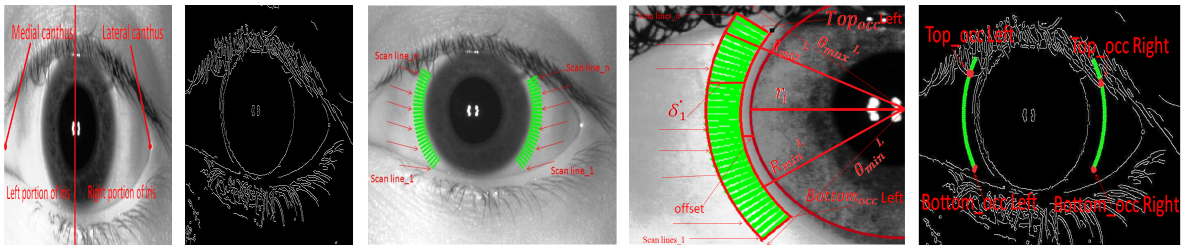

(a) Original Img. (b) Edge Map. (c) Scan-lines. (d) Annotated. (e) Top/Bot Occl. (L/R)

Figure 1: Overview of Occlusion Exclusion, showing Edge Map and Left/Right Occlusion.

in (Kywe et al., 2006) to detect contact lens using temperature variations. Basic edge extraction algorithms has been utilized in (Erdogan and Ross, 2013) to detect abrupt intensity changes and to extract contact lens border. Texture features has been utilized in (Yadav et al., 2014; Kohli et al., 2013) to obtain impressive contact lens detection performance. Some recent previous results are tabulated in Table 1.

Table 1: Previous Work on Soft Contact Lens Detection.

Cite	Technique Used	Database	Result
(Kywe et al., 2006)	Thermo-Vision	39 Subject	50-66%
(Erdogan and Ross, 2013)	Edge Detection	ICE 2005	72-76%
		MBGC	68.8-70%
(Yadav et al., 2014)	Texture Features	IIITD Cogent	56.66%
		IIITD Vista	67.52%
		UND I(2013)	65.41%
		UND II(2013)	67%

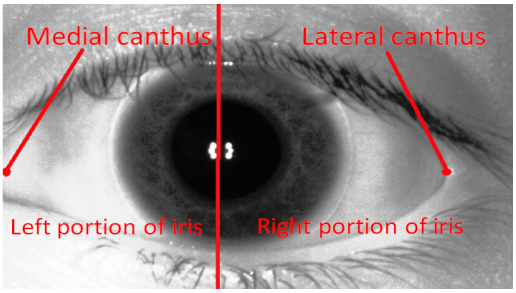

Figure 2: Original Annotated Image.

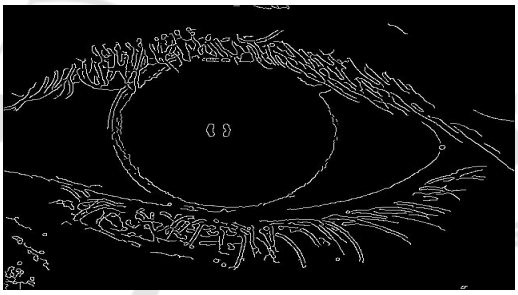

Figure 3: Edge Map of Original Image.

2 OCCLUSION EXCLUSION FROM LENS

Eyelids and eyelashes are two major challenges in detecting contact lens as they occlude significant iris regions. Particularly eyelid occlusion detection helps to set dynamic angle range which depends on the visibility of contact lens as lens cannot be beyond the eyelid boundaries. We detect occlusion from contact lens area using Canny edge detector with a high threshold (an overview of occlusion exclusion is shown in Fig. 1). Since sclera is white and texture-less there cannot be any edge points. If some edge points are present on sclera they must be due to eyelashes and eyelids. Based on these edge points dynamic angle range is defined ensuring that our algorithm never crosses the eyelid boundaries.

Iris image I is segmented by algorithm proposed in (Bendale et al., 2012), that uses Hough transform and Integro differential operator to obtain center (C_x,C_y) and the distance between center to limbus boundary r_i. An edge map of iris image using Canny is generated using higher threshold and false edges are removed by excluding those connected component that are less than P pixels in size as shown in Figure 3. Now an arrangement of scan-lines (Fig. 4) is characterized with in the radius range $\{R^L_{min}$ to $R^L_{max}\}$ and $\{R^R_{min}$ to $R^R_{max}\}$ for left and right iris portion respectively, as shown in Figure 5 and defined below:

$$R^L_{min} = (r_i + \delta_1 + offset) \quad (1)$$
$$R^L_{max} = (R^L_{min} + \delta_3) \quad (2)$$
$$R^R_{min} = (r_i + \delta_2 + offset) \quad (3)$$
$$R^R_{max} = (R^R_{min} + \delta_4) \quad (4)$$

where, δ_1, δ_2 are the difference between the maximum possible radius of the lens and minimum possible radius of iris for left and right iris portions respectively. The values of δ_3, δ_4 are discussed in next subsection. The details of occlusion exclusion procedure has been given in Algorithm 1, used to estimate Top_{occ} and $Bottom_{occ}$ as shown in Fig. 6.

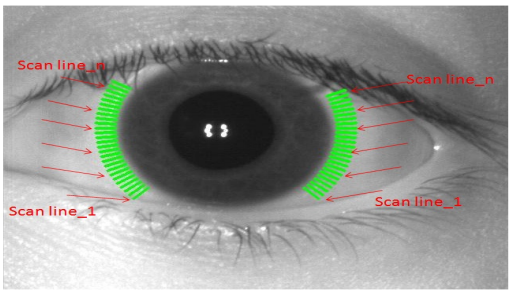

Figure 4: Scan Line Arrangement.

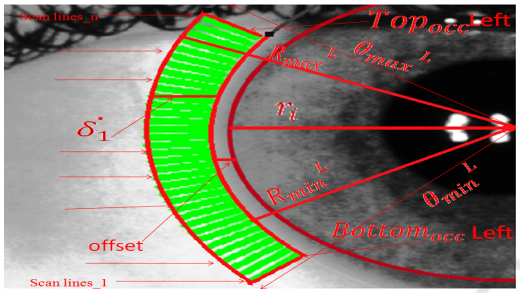

Figure 5: Annotated Image version.

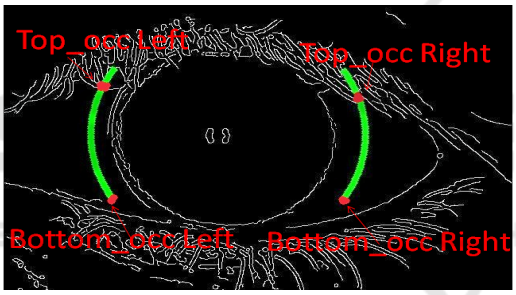

Figure 6: Top and Bottom Occlusion (Left/Right) portion.

2.1 Parameter Selection

Human iris diameter lies in the range of 10.2 to 13.0 *mm* with its expected value as *12 mm* (Caroline and Andre, 2002) whereas soft contact lens diameter ranges from 13*mm* to 15*mm* (Details-a, 2010). However, diameter of an iris fluctuates from *4 to 8 mm* in the dark and *2 to 4 mm* in bright light (Details-b, 2010). For calculating δ_1 and δ_2, *1 mm* is assumed to be equivalent to *3.779 pixels*. Ideally based on heuristics δ_1 (in pixels) should be equal to 3.779 times the difference between maximum possible contact lens radius and minimum possible iris radius. But due to dark and bright/light effect it can be much more. For this work it is observed that they can vary from 25 to 35 pixel for UND, IIITD-Cogent, IIIT-Vista and IITK contact lens databases. Ideally $\delta_1 = \delta_2$, but the lens may be misplaced or shifted towards left or right. In case of right shifting, δ_2 is greater than δ_1 and vice-versa. Also, empirically δ_3 and δ_4 values depending on visible part of contact lens can be fixed. Experimentally they are found to follow: $offset \geq 0$ and δ_3 ,$\delta_4 \in \{1,10\}$. If δ_3, δ_4 are greater than 10, then one have to shrink our angle range because we are going toward medial canthus or lateral canthus as shown in Figs 2, 5 which will degrade the accuracy substantially.

Algorithm 1: Occlusion Exclusion from Lens Area.

Require: I: Iris image, (C_x, C_y, r_i): center and radius.
Ensure: $Bottom_{occ}$: Minimum range of θ, Top_{occ}: Maximum range of θ.

Part A: Define

θ^L_{min},θ^R_{min}: $(5*\frac{\pi}{4}),(\frac{\pi}{4})$ //min angle for left,right
θ^L_{max},θ^R_{max}: $(7*\frac{\pi}{4}),(3*\frac{\pi}{4})$ //max angle for left,right
R^L_{min}: $(r_i+\delta_1+offset)$ //min radius for left
R^L_{max}: $(R^L_{min}+\delta_3)$ //max radius for left
R^R_{min}: $(r_i+\delta_2)$+offset //min radius for right
R^R_{max}: $(R^R_{min}+\delta_4)$ //max radius for right
S: S is 1-D array used to store current scan line for corresponding θ, for given range.
$H(\theta)$: H is 1-D Array to store number of non zero entries corresponding scan line.

Part B: Steps

I_E : Edge map of (I) using canny edge detector // False edges are eliminated from an edge map by removing small connected component (having pixels less than P).
for $\theta = \theta_{min}:\theta_{max}$ **do**
// $\theta_{min}=\theta^L_{min}$, $\theta_{max}=\theta^L_{max}$ for left side and $\theta_{min}=\theta^R_{min}$, $\theta_{max}=\theta^R_{max}$ for right side.
  $count$=0;
  for $r = R_{min}:R_{max}$ **do**
// $R_{min}=R^L_{min}$, $R_{max}=R^L_{max}$ for left side and $R_{min}=R^R_{min}$, $R_{max}=R^R_{max}$ in case of right side.
    $a = C_x+r\times\cos\theta$
    $b = C_y+r\times\sin\theta$
    if(I_E(a,b)!=0)
    count = count+1
    end if
  end for
  if($count \geq T$) // T is threshold which varies database to database.
  $H(\theta)$ =1
  else
  $H(\theta)$ =0
end for
[$Bottom_{occ}$,Top_{occ}] = MaxMargin(H)
// Find the index in array H containing the maximum number of consecutive zeros and return its corresponding index angles
return ($Bottom_{occ}$,Top_{occ})

These scan-lines are within a radius range as discussed above, as well as they are also with in an angular region ranging from $\{\theta^L_{min} = \frac{5*\pi}{4}$ to $\theta^L_{max} = \frac{7*\pi}{4}\}$ and $\{\theta^R_{min} = \frac{\pi}{4}$ to $\theta^R_{max} = \frac{3*\pi}{4}\}$ for left and right iris portion respectively, with an angular distance of 1° between any two consecutive scan lines (as shown in Figure 5). Hence we are working on specified annular region of thge binary edge-map to estimate the top and bottom occlusion.

Observation: The scan-line over sclera have very few edge pixels, on the other hand if current scan-line intersects eyelashes or eyelid then it is bound to have non-zero edge pixels. Hence for each scan-line (say at an angle θ) count the number of edge (non-zero) pixels. If this count is greater then a threshold T then that scan-line is occluded else it is not occluded.

In order to estimate top and bottom occlusion angle, we computed two maximally distant (in terms of angular distance) scan-lines between which each and every scan-line is having edge pixels less than T (*i.e* not occluded). The lower angle is called $Bottom_{occ}$ which represent lower eyelid or eyelashes and the higher index angle called Top_{occ} which represent the upper eyelid or eyelashes as shown in Figure 6.

3 SOFT CONTACT LENS DETECTION

Soft contact lens detection is very challenging and only available hint is the faint lens boundaries. Hence the proposed *SCLD* algorithm uses Multi Scale Line Tracking $(MSLT)$ Algorithm (Vlachos and Dermatas, 2010), which was initially used to segment retinal vessels. This algorithm can detect very faint edges and can extract soft contact lens boundaries. The steps involved in *MSLT* algorithm are given in Algorithm 2.

Output of *MSLT* gives lines of variable size and diameter based on the visibility of the contact lens border. *MSLT* algorithm returns a binary image in which the lens border lines are clearly visible on the sclera portion, if contact lens is present as shown in Figures 7 and 8. There must be some edge-lines due to the presence of eyelid/eyelashes. Hence occlusion exclusion from contact lens area is done as discussed in Section 2. After applying *MSLT* algorithm we compute two feature *viz.* Maximum edge line Maximum Hough Votes, that are used to detect contact lens as discussed below.

An arrangement of arc-lines (scan-lines are radially outward in horizontal direction Figure 4) as shown in Figure 9(a) are characterized (arc-lines are

Algorithm 2: Steps involved in MSLT Algorithm (Vlachos and Dermatas, 2010).

1: Brightness Normalization.
2: Automated selection of initial seed pixels.
3: Initialize confidence array for boundary tracking.
4: Populating confidence array by adding most suitable boundary pixels.
5: Repeat this process for each scale. (Multi-scale boundary tracking)
6: Initial rough estimation of boundary network.
7: Smoothing using Median filter to remove irregularities.
8: Finally morphological directional filtering is performed in five different directions.

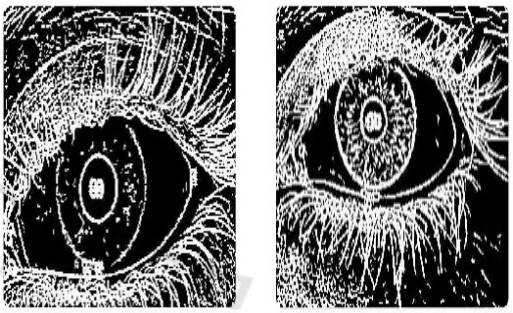

Figure 7: MSLTA algorithm based Masks (No Lens).

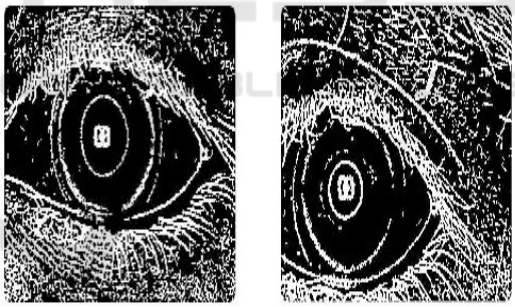

Figure 8: MSLTA based Masks (Soft Contact Lens).

vertical along an arc at some angle and radius) in an angular range of $\{\theta^L_{min}$ to $\theta^L_{max}\}$ and $\{\theta^R_{min}$ to $\theta^R_{max}\}$ for left and right iris portions respectively, at 1° angular distance. These arc-lines are of radius ranging from $\{R^L_{min}$ to $R^L_{max}\}$ form left and $\{R^R_{min}$ to $R^R_{max}\}$ for right portion at an angular distance of 1° between any two consecutive arc-line as shown in Figure 9(b) and discussed in previous Section for scan-lines. Every arc-line between an angle range of $\{Bottom_{occ}$ to $Top_{occ}\}$ is considered since it is not occluded. Algorithm 3 can be used to detect soft contact lens using line tracking.

3.1 Feature Computation

Out of all arc-line the one which has got the maximum

Algorithm 3: Soft Contact Lens Detection (SCLD) using Line Tracking.

Require: I: Iris image, (C_x, C_y): Iris Center , r_i: Iris radius, $Bottom_{occ}$, Top_{occ}.

Ensure: Two parameter, $H1$: Max Hough Voting,$Max_{linesize}$: Size of the contact lens in contact lens iris image.

Define:

θ^L_{min}, θ^R_{min}: $(5*\frac{\pi}{4}),(\frac{\pi}{4})$ //min angle for left and right side.
θ^L_{min}, θ^R_{min}: $(7*\frac{\pi}{4}),(3*\frac{\pi}{4})$ // max angle for left and right side.
R^L_{min}: (r_i)+offset //min radius for left side.
R^L_{max}: $(r_i+\delta_1)$ //max radius for left side.
R^R_{min}: (r_i)+offset //min radius for right side.
R^R_{max}: $(r_i+\delta_2)$ //max radius for right side.

Steps:

I:Apply Gaussian filter on (I)
$I1$:Apply MLSTA Algorithm(I) (Vlachos and Dermatas, 2010).
$H1$=0,$Max_{linesize}$=0.
for $r = R_{min}$:R_{max} **do** // R_{min}=R^L_{min}, R_{max}=R^L_{max} in case of left side and // R_{min}=R^R_{min}, R_{max}=R^R_{max} in case of right side.
  count=0;
  for $\theta = \theta_{min}$:θ_{max} **do** // θ_{min}=θ^L_{min}, θ_{max}=θ^L_{max} in case of left side and // θ_{min}=θ^R_{min}, θ_{max}=θ^R_{max} in case of right side.
    if($\theta \geq Bottom_{occ}$ and $Top_{occ} \geq \theta$) // Considering lines within the range // of top and bottom occlusion
      $a = C_x + r \times \cos\theta$.
      $b = C_y + r \times \sin\theta$.
      if($I1$(a,b)!=0)
        count = count+1 //Store corresponding Co-ordinate into x_i,y_i // and radius into r_1.
      end if
    end if
  end for
  $Max_{linesize}$=max($Max_{linesize}$,count) //Store corresponding $Max_{linesize}$ Co-ordinate and r into X_i,Y_i Co-ordinate and R_1.
end for
[H1] = Hough Voting(X_i,Y_i,R_1);
return ($H1$,$Max_{linesize}$)

number of edge pixels (MEP) (pixels that are probable candidates of lens) has been selected, and the

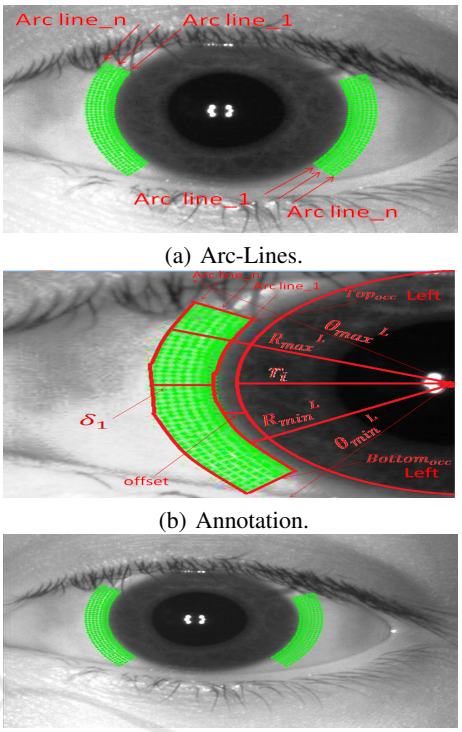

(a) Arc-Lines.

(b) Annotation.

(c) Left/Right Reg.

Figure 9: Arc-line Arrangement.

value of MEP is used as our first feature. Also to ensure circular shape Hough voting is used. The center and radius for which maximum number of Hough votes (MHV) are obtained has been selected, and the value of MHV is used as the second feature. These features can be seen as a likelihood of soft contact lens. Both MEP and MHV values must be high in case of soft contact lens and vice-versa as shown in Figure 10. The overall flow diagram of the complete Soft Contact Lens Detection (SCLD) is shown in Figure 11.

Algorithm 4 can be used to perform Hough voting in order to extract features. All parameters used in this experimentation are reported in Table 2.

4 EXPERIMENTAL ANALYSIS

In this section experimental analysis of the proposed system is presented.

4.1 Dataset

The system performance is tested over IIITD (Yadav et al., 2014; Kohli et al., 2013), UND and self created contact lens databases, acquired using $FA2$ and

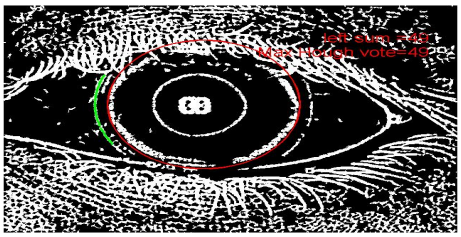

(a) Soft Contact Lens.

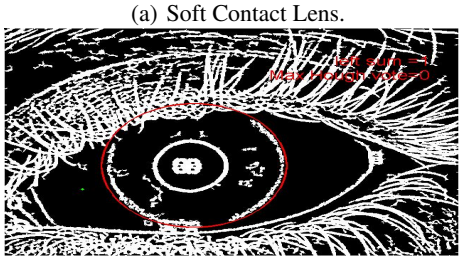

(b) No Contact Lens.

Figure 10: Pixels selected using *MEP* and *MHV* features.

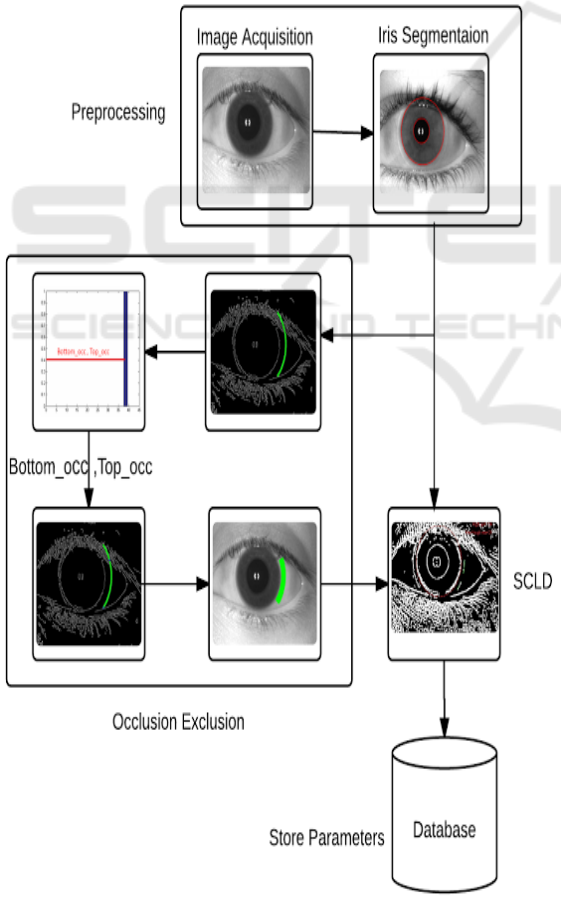

Figure 11: Soft Contact Lens Detection(SCLD) using Line Tracking.

$LG-4000$ iris sensors. The images are acquired in 3 conditions:

Algorithm 4: Hough Voting.

Require: (X_i, Y_i): Co-ordinate of the selected line, R_1: Radius of selected line

Ensure: $H1$: Max Hough Voting pixel from accumulator array.

Steps:

1: **for** every edge pixel (X_i, Y_i) **do**
2: **for** each possible radius value R_1 **do**
3: **for** each possible gradient direction Θ **do** //or use estimated gradient at (X_i, Y_i).
4: $a = X_i - r*\cos\Theta$
5: $b = Y_i + r*\sin\Theta$
6: H[a,b,r]+=1;
7: **end for**
8: **end for**
9: $H1$=max(H) //Select maximum voting pixel
10: **end for**
11: return ($H1$)

Table 2: Description of Parameter Values.

Algorithm	Parameter	Description	Value
Parameter common to all algorithm	r_i	Iris radius(in pixel)	(Bendale et al., 2012)
	(C_x, C_y)	Iris Center(in pixel)	(Bendale et al., 2012)
	δ_1, δ_2	δ_1 , δ_2 (in pixels) is the difference between the maximum possible radius of the lens and minimum possible radius of the iris, where radius of contact lens and iris in *millimeter(mm)*.	25 - 35
	δ_3, δ_4	Constant fix by experimental analysis (in pixels)	0-10
	$offset$	Constant fix by experimental analysis (in pixels)	0-10
1.Occlusion Exclusion in Contact Lens Area. 2.Soft Contact Lens Detection (SCLD) using Line Tracking.	θ: $[\theta_{min}, \theta_{max}]$	Scan line interval	$[5*\frac{\pi}{4}, 7*\frac{\pi}{4}]$ for left portion of iris $[\frac{\pi}{4}, 3*\frac{\pi}{4}]$ for right portion of iris
			$[5*\frac{\pi}{4}, 7*\frac{\pi}{4}]$ for left portion of iris $[\frac{\pi}{4}, 3*\frac{\pi}{4}]$ for right portion of iris
	r: $[R_{min}, R_{max}]$	Scan line size	$[r_i+\delta_1+offset, r_i+offset+\delta_1+\delta_3]$ for left portion of iris. $[r_i+\delta_1+offset, r_i+offset+\delta_1+\delta_3]$ for right portion of iris
			$[r_i+offset, r_i+\delta_1]$ for left portion of iris. $[r_i+offset, r_i+\delta_2]$ for right portion of iris.

- Soft contact lens iris images ['Y']
- Colored/Textured lens iris images ['C']
- Normal iris images without lens ['N']

We have only considered no contact lens and soft contact lens images *i.e.* ['N','Y'] classes and binary classification has been done. The features values as define earlier as *MEP* and *MHV* are computed for

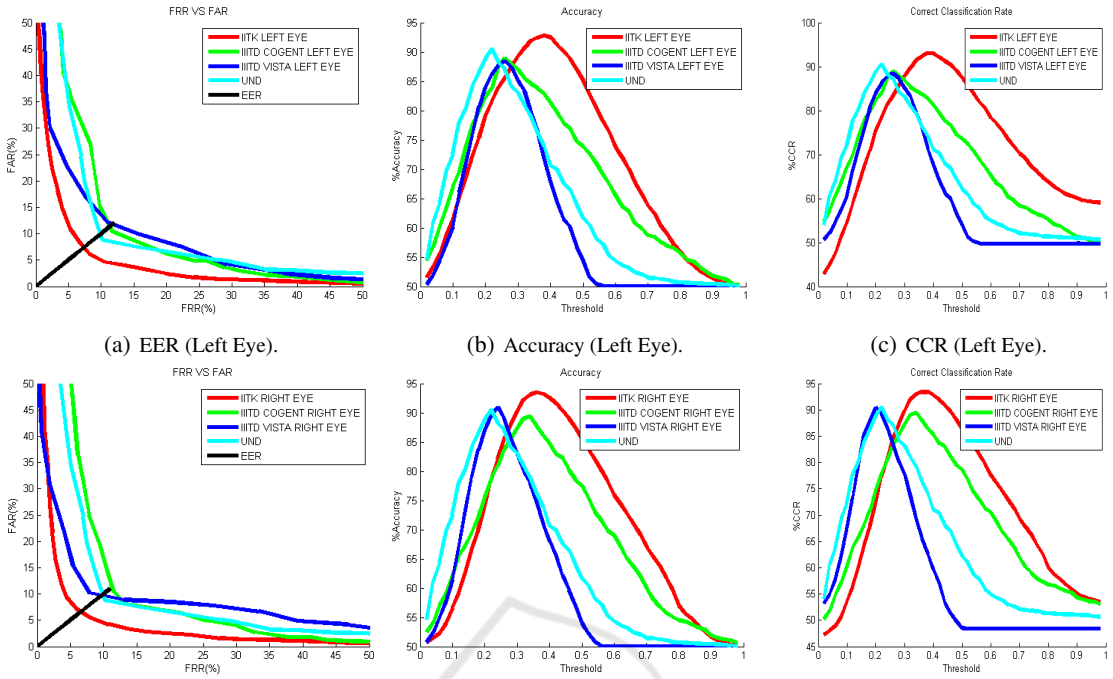

(a) EER (Left Eye). (b) Accuracy (Left Eye). (c) CCR (Left Eye).

(d) EER (Right Eye). (e) Accuracy (Right Eye). (f) CCR (Right Eye).

Figure 12: Comparative Analysis for both eyes.

every image. Their values are normalized so as to define a weighing scheme that can give a single score, ranging between $\{0$ to $1\}$. Finally this normalized weighted score is used for contact lens detection.

4.2 Threshold Selection

In order to estimate the best possible thresholding parameters all databases are partitioned into two parts, training and testing. Best suited threshold value for the above mentioned normalized weighted score is computed over the training images by checking every value with in the range of $\{0$ to $1\}$. Finally, the value of threshold at which the system performance got maximized (T_{best}), over training data, has been used for testing the proposed system over test dataset.

Prediction: Left over 34% data has been used as testing dataset. In the similar way as defined above, weighted normalized feature score has been calculated and compared against pre-computed threshold value T_{best}, for contact lens decision making.

The system performance is analyzed using standard parameters *viz.* CCR, Accuracy, FRR, FAR, EER and shown in Table 3. Accuracy is defined as $100 - \frac{FAR+FRR}{2}$. To best of our knowledge this is the first work performing two class binary classification to detect soft contact lens over IIITD Vista, IIITD Cogent and UND database hence there is no available al-

Table 3: Performance Analysis across Various databases using SCLD Line Tracking approach.

Descriptor	SCLD using Line Tracking				
Database	CCR	Accuracy	FAR	FRR	EER
IITK Left Eye	**92.99**	**92.81**	6.21	8.15	**7.56**
IITK Right Eye	**93.39**	**93.43**	7.25	5.86	**6.56**
IIITD Vista Left Eye	88.44	88.43	12.1951	10.94	**11.56**
IIITD Vista Right Eye	90.99	90.94	10.22	7.88	**9.05**
IIITD Cogent Left Eye	88.96	88.96	10.40	11.66	**11.03**
IIITD Cogent Right Eye	89.48	89.35	10.41	11.49	**10.95**
UND	90.54	90.53	8.77	10.16	**9.46**

gorithm to compare. The EER and accuracy on these database using soft contact lens detection using Line Tracking algorithm is shown in Table 3 and in Figures 12. It is observed that proposed system can handle small amount of uneven illumination also. The EER over our database has been found to be low as it is collected under controlled environmental conditions.

5 CONCLUSION

In this work fully automatic soft contact lenses detection algorithm is proposed using NIR sensor. The lens border is detected by considering small annular ring-like area near the outer iris boundary and locating candidate points while traversing along the lens

perimeter. Multi-Scale Line Tracking (MSLT) based faint edge detection algorithm is used and features like number of edge pixels (MEP) and number of Hough votes (MHV) are used for classification. Experiments are conducted on publicly available IIITD-Vista, IIITD-Cogent, UND 2010 and our indigenous database. Results of the experiment indicate that proposed method outperforms previous soft lens detection techniques.

ACKNOWLEDGEMENTS

Authors would like to thank Indian Institute of Technology Mandi and IITK for providing funds, intellectual help and guidance.

REFERENCES

Badrinath, G., Nigam, A., and Gupta, P. (2011). An efficient finger-knuckle-print based recognition system fusing sift and surf matching scores. In *Information and Communications Security*, volume 7043 of *Lecture Notes in Computer Science*, pages 374–387. Springer Berlin Heidelberg.

Bendale, A., Nigam, A., Prakash, S., and Gupta, P. (2012). Iris segmentation using improved hough transform. In *Emerging Intelligent Computing Technology and Applications*, volume 304 of *Communications in Computer and Information Science*, pages 408–415. Springer Berlin Heidelberg.

Caroline, P. and Andre, M. (2002). The effect of corneal diameter on soft lens fitting, part 2. *Contact Lens Spectrum*, 17(5):56–56.

Details-a (2010). Soft Contact Lens Diameter. Accessed: 2015-5-13.

Details-b (2010). Biometrics Data Sets. http://www3.nd.edu/∼cvrl/CVRL/Data_Sets.html. Accessed: 2015-06-5.

Erdogan, G. and Ross, A. (2013). Automatic detection of non-cosmetic soft contact lenses in ocular images. In *SPIE Defense, Security, and Sensing*, pages 87120C–87120C. International Society for Optics and Photonics.

Flom, L. and Safir, A. (1987). Iris recognition system. US Patent 4,641,349.

Kohli, N., Yadav, D., Vatsa, M., and Singh, R. (2013). Revisiting iris recognition with color cosmetic contact lenses. In *Proceedings of International Conference on Biometrics (ICB)*, pages 1–7. IEEE.

Kywe, W. W., Yoshida, M., and Murakami, K. (2006). Contact lens extraction by using thermo-vision. In *18th International Conference on Pattern Recognition (ICPR)*, volume 4, pages 570–573. IEEE.

Lovish, Nigam, A., Kumar, B., and Gupta, P. (2015). Robust contact lens detection using local phase quantization and binary gabor pattern. In *16th International Conference Computer Analysis of Images and Patterns, CAIP 2015, Valletta, Malta, September 2-4*, pages 702–714.

Nigam, A. and Gupta, P. (2011). Finger knuckleprint based recognition system using feature tracking. In *Biometric Recognition*, volume 7098 of *Lecture Notes in Computer Science*, pages 125–132. Springer Berlin Heidelberg.

Nigam, A. and Gupta, P. (2012). Iris recognition using consistent corner optical flow. In *11th Asian Conference on Computer Vision, Daejeon, Korea, November 5-9, 2012, Revised Selected Papers, Part I*, pages 358–369.

Nigam, A. and Gupta, P. (2013a). Multimodal personal authentication system fusing palmprint and knuckleprint. volume 375 of *Communications in Computer and Information Science*, pages 188–193.

Nigam, A. and Gupta, P. (2013b). Quality assessment of knuckleprint biometric images. In *20th International Conference on Image Processing (ICIP)*, pages 4205–4209.

Nigam, A. and Gupta, P. (2014a). Multimodal personal authentication using iris and knuckleprint. In *Intelligent Computing Theory*, volume 8588 of *Lecture Notes in Computer Science*, pages 819–825. Springer International Publishing.

Nigam, A. and Gupta, P. (2014b). Palmprint recognition using geometrical and statistical constraints. In *2nd International Conference on Soft Computing for Problem Solving (SocProS 2012), December 28-30, 2012*, volume 236 of *Advances in Intelligent Systems and Computing*, pages 1303–1315. Springer India.

Nigam, A. and Gupta, P. (2014c). Robust ear recognition using gradient ordinal relationship pattern. In *Computer Vision - ACCV 2014 Workshops - Singapore, Singapore, November 1-2, 2014, Revised Selected Papers, Part III*, pages 617–632.

Nigam, A. and Gupta, P. (2015). Designing an accurate hand biometric based authentication system fusing finger knuckleprint and palmprint. *Neurocomputing*, 151, Part 3:1120 – 1132.

Nigam, A., T., A., and Gupta, P. (2013). Iris classification based on its quality. In *Intelligent Computing Theories*, volume 7995 of *Lecture Notes in Computer Science*, pages 443–452. Springer Berlin Heidelberg.

Vlachos, M. and Dermatas, E. (2010). Multi-scale retinal vessel segmentation using line tracking. *Computerized Medical Imaging and Graphics*, 34(3):213–227.

Yadav, D., Kohli, N., Doyle, J., Singh, R., Vatsa, M., and Bowyer, K. W. (2014). Unraveling the effect of textured contact lenses on iris recognition. *IEEE Transactions on Information Forensics and Security*.